# Destabilization of Beta-induced Alfvén Eigenmodes in the HL-2A Tokamak

W. Chen*, X.T. Ding, Yi. Liu, Q.W.Yang, X.Q. Ji, Y.P. Zhang, Y.B. Dong, Y. Huang, J. Zhou, Y. Zhou, W. Li, B. B. Feng, X.M. Song, J.Q. Dong, Z.B. Shi, X.R. Duan, and HL-2A team.

Southwestern Institute of Physics, P.O.Box 432 Chengdu 610041, China
E-mail contact of main authors: chenw@swip.ac.cn

**Abstract:** It is presented that the experimental results are correspond to the Beta-induced Alfvén eigenmode (BAE) during a strong tearing mode activity in this paper. The BAE excited by energetic electrons (termed as e-BAE) has been identified for the first time both in the Ohmic and ECRH plasma in HL-2A. The hard X-ray (HXR) spectrum detected by Cadmium-telluride (CdTe) and the non-thermal radiation measured by the ECE are used to analyze the behaviors of the energetic electrons. Experimental results show that the e-BAE is related not only with the populations of the energetic electrons, but also their energy distribution. To assess the identification of these instabilities with the BAE modes, the generalized fishbone-like dispersion relation (GFLDR) and magnetic-island-induced BAE dispersion relation have been solved near marginal stability, respectively. Comparing with experimental results, the calculation analysis shows that the observed frequencies are all close to the theoretical results.

## 1. Introduction

Alfvénic instabilities can be driven by the energetic particle in future burning plasma devices, such as ITER and DEMO, where energetic particles will be abundantly produced by high power heating and fusion reaction. These instabilities can lead to significant loss of energetic particles, which are very harmful for plasma heating and reactor's first wall. So it is very important to study them theoretically and experimentally in present day tokamak plasmas. The instabilities driven by fast ions, such as toroidicity-induced Alfvén eigenmodes (TAEs), have been observed and investigated widely in many fusion devices [1]. In constrast, the modes related to energetic-electrons are much less explored. The study of energetic-electron behaviors would provide a strong contribution to the physics of burning plasma because their effect on low-frequency MHD modes can be used to simulate and analyze the analogous effect of alpha particles characterized by small dimensionless orbits similar to energetic-electrons in present day tokamak plasmas [2].

The BAEs were firstly observed in DIII-D and then TFTR plasmas with fast ions [3-5]. Subsequently, the BAEs (termed as m-BAEs) have also been observed during a strong tearing mode (TM) activity in FTU and TEXTOR Ohmic plasmas without fast ions [6-8]. Recently, the BAEs have also been reported during a sawtooth cycle in ASDEX-U and TORE-SUPRA plasmas with fast ions [9-10]. The excitation mechanism of the BAEs is not well understood due to many effects, such as ion diamagnetic drift, thermal ion compression, finite Larmor radius (FLR)/finite orbit width (FOW), and energetic-particle effects. The most probable theoretic identifications of the BAE excited by beam ions have been proposed: a discrete shear Alfvén eigenmode (AE), a kinetic ballooning mode (KBM) and a hybrid mode between Alfvénic and KBM branches or between Alfvénic and ion acoustics branches [11-12].

In this paper, it is reported that experimental results are correspond to the m-BAEs. It is present for the first time that the experimental results are associated with the e-BAEs in ECRH and low density Ohmic plasmas. In order to assess the identification of these instabilities with the BAE modes, the BAE dispersion relations have been solved under near marginal stability. Comparing with experimental results, the calculation analyses show that the observed frequencies are all close to the theoretical results.

## 2. Experimental observations

HL-2A is a medium-size tokamak with major radius $R=1.65m$ and minor radius $a=0.4m$ [13]. The experiments discussed here have been performed in deuterium plasmas with toroidal plasma current $I_p=160/300kA$, toroidal field $B_t=1.3/2.4T$, safety factor at the edge $q_a\approx 4.0$, and electron cyclotron resonance heating (ECRH) as the main heating. The magnetic fluctuations are followed by Mirnov probes and soft X-ray arrays. The line averaged density is detected by a hydrogen cyanide interferometer. The electron and ion temperature is measured by the Tomson laser scattering (TLS) and neutral particle analyzer (NPA), respectively. The hard X-ray (HXR) spectrum detected by Cadmium-telluride (CdTe) and the non-thermal radiation measured by the ECE are used to analyze the behaviors of the energetic electrons.

### 2.1 BAEs excited by large magnetic islands

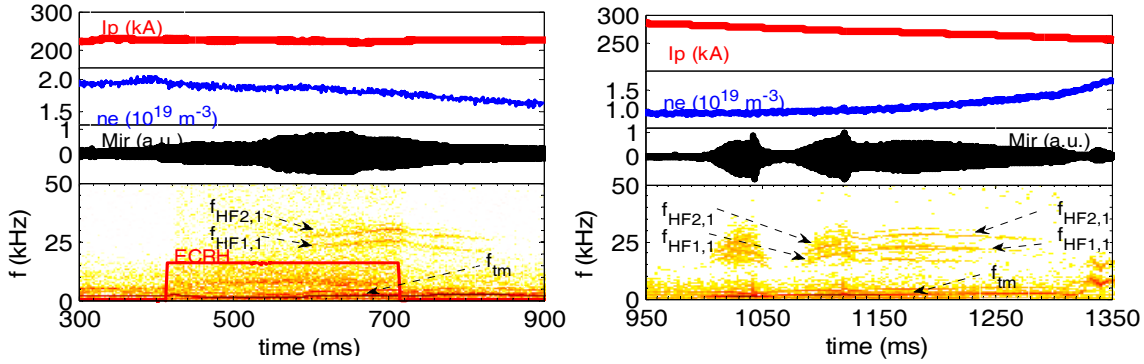


Figure 1. Spectrograms of Mirnov signals for shots #11014 (left) and #10943 (right).

The m-BAEs have been observed on HL-2A, recently, and the characteristics of the m-BAEs have been investigated [14]. The spectrogram of a Mirnov-coil signal has revealed the existence of high-frequency (f~15-35 kHz) instability (HFI) in Ohmic or ECRH plasmas, and the HFIs can be observed during current-plateau and current-ramp-down phases (shown in figure 1) . Note that these typical data are selected for latter analysis. From Fig.1, it is seen that the lower frequency modes ($0<f<5$ $kHz$) present m/n=2/1 magnetic islands and last a long time, and the tearing modes propagate poloidally in the electron diamagnetic drift direction. At the interval of $600\ ms<t<800\ ms$ for shot 11014 and $1000\ ms<t<1250\ ms$ for shot 10943, the intensity of the magnetic signals increases and the HFIs are driven. It is evident that the HF modes occur in pairs. The frequencies of the HFIs decrease after the ECRH is switched off at $t=714\ ms$. At $t=1040\ ms$ and $1120\ ms$ for shot 10943, there are two internal disruptions, and the island amplitude attenuates with disruption and increases subsequently. The pair modes have maximum amplitudes at $t\simeq 714\ ms$ for shot 11014, $t\simeq 1040\ ms$ and $1120\ ms$ for shot 10943,

and the root mean square (RMS) of island amplitude is about $10^{-4}-10^{-3}$. The frequency difference $\Delta f$ between the pair modes is exactly twice the fundamental frequency $f_{tm}$ of the tearing modes, namely, $\Delta f = f_{HF\,2,1} - f_{HF\,1,1} = 2\,f_{tm}$.

In the island rest frame, the mode frequencies and mode numbers have different algebraic signs. It is determined the $f_{HF\,2,1}$ and $f_{HF\,1,1}$ modes have different mode number m/n=-2/-1 (co-rotation with an island) and m/n=2/1 (counter-rotation with an island), respectively, and the HFIs represent a pair of counter-propagating waves and form a standing-wave structure.

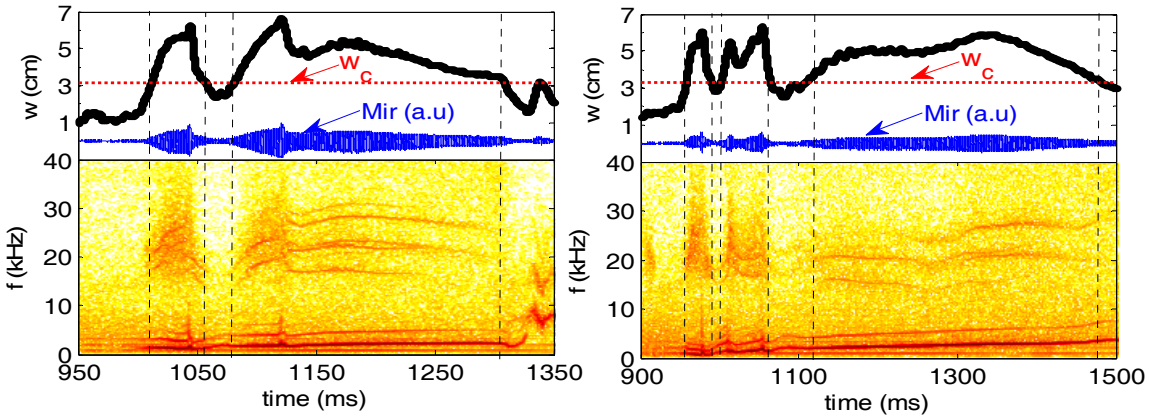


Figure 2. Evolutions of magnetic island width and mode frequency for shots #10943 (left) and #10981 (right)

The magnetic island structure in HL-2A has been investigated [15]. The perturbation currents as the source of the perturbation flux can be determined by Mirnov coils. By superposing the perturbation flux and equilibrium flux reconnected by the EFIT code, the structure and width of the magnetic islands can be determined. Figure 2 shows that the time evolutions of magnetic island widths and mode frequencies for different discharges. It can be found that the width islands $w$ are about 3-7 cm during a strong tearing mode activity. And there is an island width threshold for the mode excitation. The modes can be driven when the width island $w$ exceeds the threshold $w_c$. The statistical analysis is performed to confirm the threshold. The statistical relationship between mode frequencies and island width is shown in Fig. 3. The experimental result indicates that the mode frequency linearly depends on the island width, and it is found that the island-width threshold $w_c$ is about 3.4 cm on HL-2A.

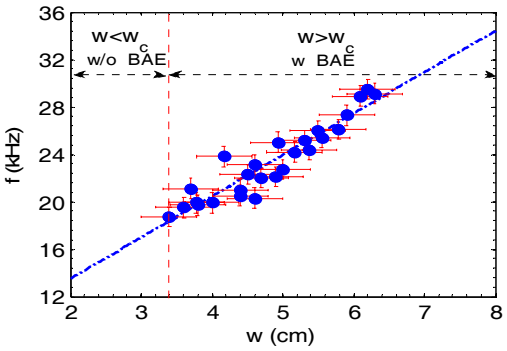


Figure 3. Mode frequency versus magnetic island width. Marker points indicate experimental data. Dashed curves show linear-fit results.

### 2.2 BAEs excited by energetic electrons

The e-BAE has been observed in the HL-2A ECRH plasma. This phenomenon is perfectly reproducible. The mode features, including its frequency, mode-number and propagation

direction, can be observed by magnetic pickup probes. Figure 4 shows a typical experimental result with low plasma density during ECRH. Electron cyclotron wave (1MW, 68GHz, second harmonic heating) is launched into the plasma with 1.3T toroidal magnetic field. Here, the plasma density, ECRH pulse, NBI pulse, magnetic fluctuation signal from Mirnov probes and its frequency spectrum have been shown from the top to the bottom. A coherent MHD fluctuation is visible around 20 kHz between 420 ms and 800 ms. The density slightly increases after NBI at t=550 ms, but the mode does not almost change. The mode becomes very weak after ECRH switched off at t=800 ms, in despite of NBI presenting at t=800-860 ms. The mode activity exhibits no amplitude bursting and frequency chirping different from electron fishbone (e-fishbone) characteristics in HL-2A [16-17]. They do not correspond to toroidal Alfven eigenmodes (TAE) because their frequencies are sharply less than TAE frequency $f_{TAE} = v_A / 4\pi qR$ ( $f_{TAE} \approx 160kHz$ for the deuterium plasma with $B_t = 1.3T$, $n_e = 0.4\times10^{19} m^{-3}$ and $q = 3$ in HL-2A). The magnetic field fluctuations measured at the wall are $B_\theta / B \sim 10^{-5} - 10^{-4}$ and have clear mode numbers $m/n = -3/-1$. The m-BAEs are also visible during strong tearing mode activity (TM) in the same discharge. Comparing with m-BAE and e-BAE, it is found that the frequency of m/n=-3/-1 mode is provided with the same order of the frequencies of the m-BAEs. The m/n=-3/-1 mode propagates poloidally parallel to the electron diamagnetic drift velocity and toroidally opposite parallel to the plasma current in the laboratory frame of reference.

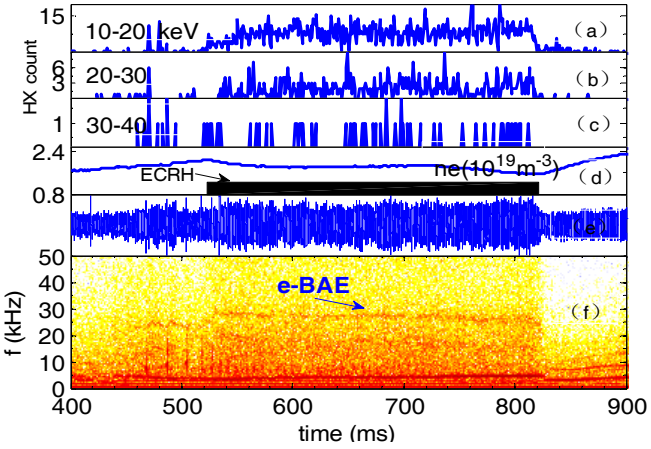


Figure 5. HL-2A shot #13364. (a-c) counts of hard x-ray (HXR) photons at different energy ranges (d) central line-average density; (e) magnetic probe signal; (f) the spectrogram of magnetic probe signal. Plasma current $I_p = 320kA$, toroidal field $B_t = 2.4T$, central electron temperature, $T_e \sim 2.3keV$, edge safety factor $q_a \approx 4.0$, and ECRH power $P_{ECRH} = 1.41MW$.

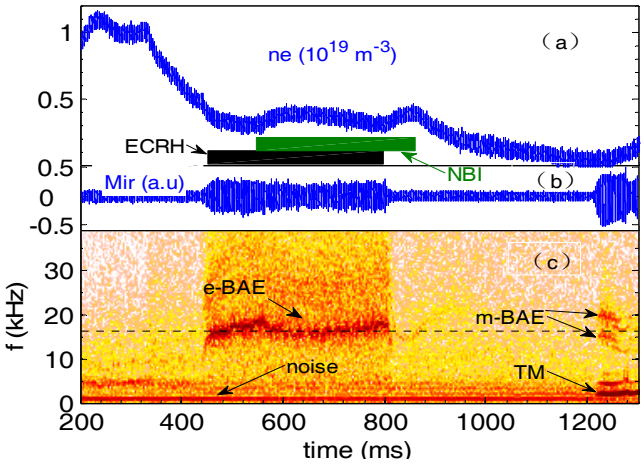


Figure 4. HL-2A shot #10579. (a) central line-average density; (b) magnetic probe signal; (c) the spectrogram of magnetic probe signal. Plasma current $I_p = 160kA$, toroidal field $B_t = 1.3T$, central ion and electron temperature $T_i \sim 0.85keV$, $T_e \sim 1.10keV$, edge safety factor $q_a \approx 4.0$, ECRH power $P_{ECRH} = 1.0MW$ and NBI power $P_{NBI} = 0.38MW$.

Figure 5 shows that the mode can also be observed on occasion in higher plasma density

and toroidal magnetic field. In this discharge, the mode can be found when the density is around $ne \approx 1.6\times10^{19} m^{-3}$ with toroidal magnetic field $B_t = 2.4T$, but the mode intensity is very weak. Figure 2 also shows that the m/n=-3/-1 mode excitation is correlated with the energetic electrons. The energy distribution of the electrons is indirectly measured by a hard X-ray detector (CdTe) with the pulse height analysis (PHA). The counts of hard x-ray photons increase largely during ECRH, and they are shown in Fig.5 (a-c). When the counts of the energetic electrons with 10-40keV increase to a higher level, the m/n=-3/-1 mode is observed. From Fig.4 and Fig.5, it is found that the energetic electrons produced by EC wave can provide the necessary energy to drive modes above the stability threshold during ECRH. The population of energetic electrons is insufficient after ECRH switched off, and can not overcome damping and not destabilize the mode unstable.

The m/n=-3/-1 mode can often be observed in low density Ohmic plasma. From Fig.6, it is found that the intensity of the mode in Ohmic plasma is weak at t=600-1200 ms, but it becomes strong during high power ECRH in the same discharge. It can be proved that the m/n=-3/-1 mode in Ohmic plasma is also excited by energetic electrons. It is well known that the electrons can be accelerated by the Ohmic electric field in tokamak plasma. Under the influence of the longitudinal electric field, the initially maxwellian electron distribution function begins to grow an energetic-electron tail. The low density discharge regime is characterized by a large energetic-electron population. When the ratio of the electron plasma frequency to the electron cyclotron frequency $\omega_{pe}/\omega_{ce} < 0.3$ according to the empirical values in several machines, the Anomalous Doppler Instability (ADI) [18-21] can be excited. For #10580 discharge with toroidal field $B_t = 1.3T$, the ADI is excited when the density is less than critical density $n_{ec} \approx 0.14\times10^{19} m^{-3}$. From Fig.6, it is found that the m/n=-3/-1 mode disappears as soon as the ADI is excited at t=1200 ms . The ADI causes pitch angle scattering of the energetic electrons. The ADI transfers energy from parallel to perpendicular motion, i.e. the circulating electrons become trapped electrons. The phenomenon indicates that the circulating energetic electrons effectively contribute to the mode excitation.

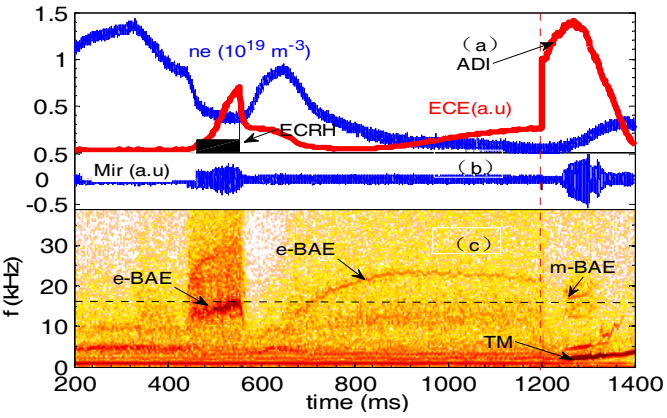


Figure 6. HL-2A shot #10580. (a) central line-average density and non-thermal radiation measured by ECE; (b) magnetic probe signal; (c) the spectrogram of magnetic probe signal. Plasma current $I_p = 160kA$, toroidal field $B_t = 1.3T$, central ion and electron temperature $T_i \sim 0.50keV$, $T_e \sim 0.62keV$, edge safety factor $q_a \approx 4.0$, and ECRH power $P_{ECRH} = 0.89MW$.

### 3. Calculation and analysis

The BAE frequency can be estimated by the continuum accumulation point (CAP) of the low frequency gap induced by the shear Alfvén continuous spectrum due to finite beta effect.

At the lowest order, the CAP is given by [22]

$$\mathrm{f}_{CAP} = \frac{1}{2\pi}\left(\frac{7}{4}+\frac{T_e}{T_i}\right)^{1/2} q\omega_{ti} \tag{1}$$

Here $\omega_{ti} = (2T_i / m_i)^{1/2} / qR$ is the ion transit frequency, $T_e$ and $T_i$ are respectively the electron and ion temperatures, and R is plasma major radius. Note that the CAP frequency only is an upper bound for the expected mode frequencies. To further identify with the BAE, the generalized fishbone-like dispersion relation (GFLDR) [23-26] developed by Zonca is given by

$$-i\Lambda(\omega) + \delta\hat{W}_f + \delta\hat{W}_k = 0 \tag{2}$$

Where $i\Lambda(\omega)$ is the inertial layer contribution due to thermal ions, while $\delta\hat{W}_f$ and $\delta\hat{W}_k$ come from fluid MHD and energetic particle contributions in the regular ideal regions. The frequency gap of shear Alfvén wave (SAW) can be given by the condition $\mathrm{Re}\,\Lambda^2 < 0$. The GFLDR is used to study plasma dynamics with the frequency range from kinetic ballooning mode (KBM)/BAE to TAE. On the basis of the GFLDR, the two types of modes exist. One is the discrete Alfvén eigenmode (AE) for $\mathrm{Re}\,\Lambda^2 < 0$. Another one is the energetic particle continuum mode (EPM) for $\mathrm{Re}\,\Lambda^2 > 0$. The combined effect of $\delta\hat{W}_f$ and $\mathrm{Re}\,\delta\hat{W}_k$ determines the existence conditions of AE by removing the degeneracy with the SAW accumulation point, and it depends on the plasma equilibrium profiles, e.g. temperature, density and safety factor. Thus, the various effects on $\delta\hat{W}_f + \mathrm{Re}\,\delta\hat{W}_k$ can lead to AE localization in various gaps, i.e. to different species of AE. When considering the kinetic effects on low mode number MHD modes, the sideband poloidal mode numbers cannot be considered degenerate and the kinetic expression of $\Lambda$ for $\omega_{bi} < |\omega| \ll \omega_A$ is given by

$$\Lambda^2 = \frac{\omega^2}{\omega_A^2}\left(1-\frac{\omega_{*pi}}{\omega}\right) + q^2\frac{\omega\omega_{ti}}{\omega_A^2}\left[\left(1-\frac{\omega_{*ni}}{\omega}\right)F - \frac{\omega_{*Ti}}{\omega}G - \frac{N_m}{2}\left(\frac{N_{m+1}}{D_{m+1}}+\frac{N_{m-1}}{D_{m-1}}\right)\right] \tag{2}$$

Where $\omega_{*pi} = \omega_{*ni} + \omega_{*Ti} = (T_i / eB)k_\theta(\nabla \ln n_i)(1+\eta)$ is ion diamagnetic drift frequency, $\omega_{*ni} = (T_i c / eB)(\vec{k}\times\vec{b})\cdot\nabla \ln n_i$, $\omega_{*Ti} = (T_i c / eB)(\vec{k}\times\vec{b})\cdot\nabla \ln T_i$, $\eta = \nabla \ln T_i / \nabla \ln n_i$, $k_\theta = -m/r$, and the functions, $F(x)$, $G(x)$, $N(x)$ and $D(x)$ are defined as $F(x) = x(x^2+3/2) + (x^4+x^2+1/2)Z(x)$, $G(x) = x(x^4+x^2+2) + (x^6+x^4/2+x^2+3/4)Z(x)$, $N(x) = (1-\omega_{*ni}/\omega)[x+(1/2+x^2)Z(x)] - (\omega_{*Ti}/\omega)[x(1/2+x^2) + (1/4+x^4)Z(x)]$, $D(x) = (1/x)(1+\tau) + (1-\omega_{*ni}/\omega)Z(x) - (\omega_{*Ti}/\omega)[x+(x^2-1/2)Z(x)]$, with $x = \omega/\omega_{ti}$, $\tau \equiv T_e / T_i$ and $Z(x) = \pi^{-1/2}\int_{-\infty}^{+\infty} e^{-y^2}/(y-x)\,dy$ the plasma dispersion function. $N_m(x)$ and $D_m(x)$ are defined as the functions $N(x)$ and $D(x)$ given above, having made explicit the poloidal mode number $m$ to be used for computing their dependences on diamagnetic frequencies. The thermal ion transit resonances as well as diamagnetic effects (finite $\omega_{*pi}$) usually provide higher order corrections to the frequency spectrum.

For the magnetic-island-induced BAE, the corresponding dispersion relation [27] is given by,

$$-2\sqrt{Q}\cdot\Gamma\left(\frac{3}{4}-\frac{\Lambda^2}{4Q}\right)/\Gamma\left(\frac{1}{4}-\frac{\Lambda^2}{4Q}\right) = \frac{|sm|\pi}{\Delta'} \tag{4}$$

$$Q^2(\omega) = s^2k_\theta^2\rho_{Li}^2\frac{\omega^2}{\omega_A^2}\left[\frac{3}{4}\left(1-\frac{\omega_{*pi}}{\omega}-\frac{\omega_{*Ti}}{\omega}\right) + q^2\frac{\omega_{ti}}{\omega}S(\omega) + \frac{(\Lambda\omega_A/\omega)^4}{1/\tau + (\omega_{*ni}/\omega)}\right] \tag{5}$$

here，all symbols are standard and they can be found in the ref. [26] and [27].

The eq. 2 and eq.4 can be solved easily near marginal stability, i.e. $|\Lambda(\omega)|=0$. In the present m-BAE experiment, the center ion temperature $Ti=0.3-0.8\ keV$, and the center electron temperature $Te=0.3-2.0\ keV$, $Ti|_{q=2}=0.2-0.4\ keV$ and $Te/Ti|_{q=2}=1-4$, where $|_{q=2}$ denotes the q=2 surface location. Using these parameters, the eq. 4 is solved and the theoretical values are shown in Fig.7. It is found that the mode frequencies $f(m=\pm2)$ are lower than $f_{cap}$, $\Delta f = f_{CAP} - f(m=\pm2) \approx (3-5)\ kHz$, and $f(m=-2) < f(m=+2)$. For $0.2<T_i<0.4\ keV$, the mode frequencies are $18<f<28\ kHz$. Apparently, the measured m-BAE frequencies are quantitatively consistent with the theoretical frequencies.

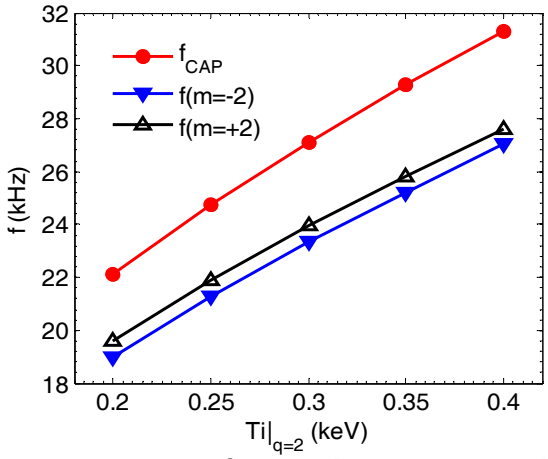


Figure 7. $f_{CAP}$ and $m=\pm2$ mode frequencies versus q=2 surface ion temperature. Other plasma parameters are $Te=1.0\ keV$, $Te/Ti|_{q=2}=1$, $s=1$, $\Delta'=4$, $\omega_{*Ti}=0.4\omega_{*pi}$, and $\omega_{*ni}=0.6\omega_{*pi}$.

In the present e-BAE experiment, we assume $B=1.3T$, and $r=32cm$, $n_e=n_i$, $\eta=1.5$ and $-R_0\nabla\ln n_i=6.0$ at the q=3 surface. We obtain $k_\theta = m/32cm \approx m\cdot3.1m^{-1}$, and $\omega_{*pi}/2\pi=(\omega_{*ni}+\omega_{*Ti})/2\pi \approx mT_i\cdot3.5kHz$. According to the parameters, the equation (2) has been solved near marginal stability ($\Lambda=0$). Fig.8 shows the frequency of the BAE accumulation point versus ion temperature at q=3 surface. Using pulse #10579 experimental data, the ion diamagnetic frequency is $\omega_{*pi}/2\pi \approx 1.6kHz$ at the q=3 surface with $T_i|_{q=3} \approx 0.15keV$. The observed frequency of the m/n=-3/-1 mode is around $f=18kHz$, while the frequency of the BAE accumulation point is around $f\approx19kHz$ ($\tau=1$) or $f\approx22kHz$ ($\tau=2$). It is obvious that the observed frequency coincides with the theoretical prediction based on the GFLDR. This analyzed result supports that the mode is the e-BAE instability.

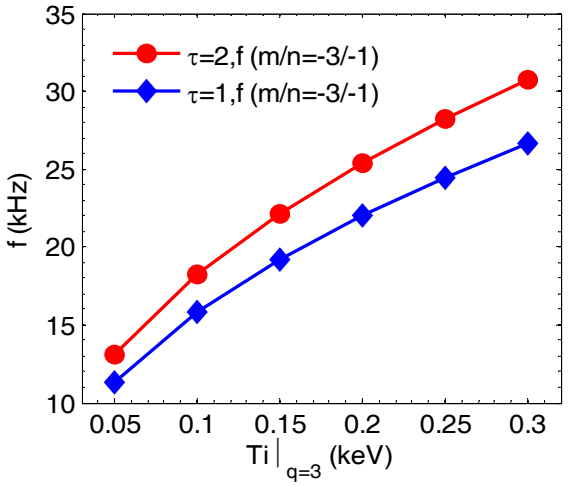


Figure 8. The frequency of the BAE accumulation point versus ion temperature at q=3 surface. (● : $\tau\equiv T_e/T_i=2$ ; ◆ : $\tau\equiv T_e/T_i=1$).

## 4. Summary

In the present study, the m-BAEs have been observed and demonstrated on HL-2A. The mode frequency ranges from 15 to 35 kHz, and it is provided with the same order of the low frequency gap induced by finite beta effects. It has been identified the modes propagate poloidally and toroidally in opposite directions, and form standing-wave structures in the island rest frame. The mode frequencies are associated with island width, and the frequency difference of the two branch modes is determined by the island rotation frequency. The

island-width threshold has been found by statistical analysis, which threshold $w_c$ is about 3.4 cm on HL-2A, and it is especially important for the m-BAE excitation. The theoretical expression of the island width is qualitative agreement with the experimental results, and it is shown that the theoretical m-BAE frequency is in quantitative consistent with the experimental results by solving the m-BAE dispersion. The experimental data presented here identify for the first time an energetic-electron-driven BAE in HL-2A. The e-BAE and m-BAE often can be observed in the same discharge, and their frequencies have the same order, i.e. $O(f_{e-BAE}) = O(f_{m-BAE})$. The evolution of energetic electrons is monitored by ECE radiometer and CdTe detector. The experimental results show that the e-BAE excitation is related not only with the populations of the energetic electrons, but also the energy and pitch angle of them. The observed mode features agree with the predictions of the GFLDR. The mode frequency is comparable with that of the CAP of the lowest frequency gap induced by the shear Alfvén continuous spectrum due to finite beta effect. The modes occur in plasmas with magnetic safety factor $q = 3$ and propagate poloidally in electron diamagnetic direction. The kinetic thermal ions effects probably are much important in process of low frequency Alfvénic fluctuation excitation.

## References


[1] A. Fasoli *et al*., Nucl. Fusion **47**, S264 (2007).
[2] F. Zonca F *et al*., Nucl. Fusion **47**, 1588 (2007).
[3] W. W. Heidbrink *et al.*, Phys. Rev. Lett. **71,** 855 (1993).
[4] R. Nazikian *et al.*, Phys. Plasmas **3,** 593 (1996).
[5] W. W. Heidbrink *et al.*, Phys. Plasmas **6,** 1147 (1999).
[6] P. Buratti *et al.*, Nucl. Fusion **45,** 1446 (2005).
[7] O. Zimmermann, *et.al.* Proc. 32nd EPS Conf. (Tarragona, Spain), P4.059 (2005).
[8] S. V. Annibaldi *et al.*, Plasma Phys. Control. Fusion **49,** 475 (2007).
[9] C.Nguyen, *et al.*, Plasma Phys. Control. Fusion **51,** 095002 (2009).
[10] P. Lauber, *et al.*, Plasma Phys. Control. Fusion **51,** 124009 (2009).
[11] S. T. Tsai and L. Chen, Phys. Fluids **B5** (1993) 3284.
[12] N. N. Gorelenkov and W. W. Heidbrink: Nucl. Fusion **42** (2002) 150.
[13] Q.W. Yang, *et al.*, Nucl. Fusion **47,** S635 (2007)
[14] W. Chen, *et al*., J.Phys.Soc.Jpn **79,** 044501 (2010).
[15] X. Q. Ji, *et al*., Plasma Sci. Technol. **8** 644 (2006).
[16] W. Chen *et al*., Nuclear Fusion **49**, 075022 (2009).
[17] W. Chen *et al.*, Nuclear Fusion **50**, 084008 (2010).
[18] H. Knoepfel and D.A. Spong, Nuclear Fusion **19**, 785 (1979).
[19] S.C. Luckhardt *et al*., Phys. Fluids **30**, 2110 (1987).
[20] P. Blanchard *et al.*, Plasma Phys. Control. Fusion **44,** 2231 (2002).
[21] H.W. Hu *et al*., Phys. Scr. **81,** 025503 (2010).
[22] F. Zonca *et al.*, Plasma Phys. Control. Fusion **38,** 2011 (1996).
[23] L. Chen *et al*., Phys. Rev. Lett. **52,** 1122 (1984).
[24] F. Zonca *et al.*, Plasma Phys. Control. Fusion **40,** 2009 (1998).
[25] S. Briguglio *et al*., Nuclear Fusion **40**, 701 (2000).
[26] F. Zonca *et al.*, Nucl. Fusion **49**, 085009 (2009).
[27] S. V. Annibaldi, F. Zonca, and P. Buratti, Plasma Phys. Control. Fusion **49**, 475(2007).